

Enhanced Emission and Analyte Sensing by Cinchonine Iridium(III) Cyclometalated Complexes Bearing Bent Diphosphine Chelators

Shao-Xiong Luo,^{†,‡,§} Lu Wei,^{†,‡,§} Xin-Hai Zhang,[†] Min Hwee Lim,[§] K. X. Vivian Lin,[†] M. H. Valerie Yeo,[†] Wen-Hua Zhang,^{*,†} Zhi-Pan Liu,^{*,†,⊥} David J. Young,^{*,†,⊥} and T. S. Andy Hor^{*,†,§}

[†]Institute of Materials Research and Engineering, Agency for Science, Technology and Research, 3 Research Link, 117602, Singapore,

[‡]Raffles Institution, 1 Raffles Institution Lane, 575954, Singapore

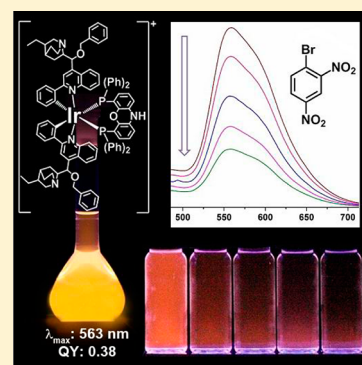
[§]Department of Chemistry, National University of Singapore, 3 Science Drive 3, 117543, Singapore

^{||}MOE Key Laboratory for Computational Physical Sciences, Fudan University, Shanghai 200433, People's Republic of China

[⊥]Faculty of Science, Universiti Brunei Darussalam, Jalan Tungku Link, Gadong BE 1410, Brunei Darussalam

Supporting Information

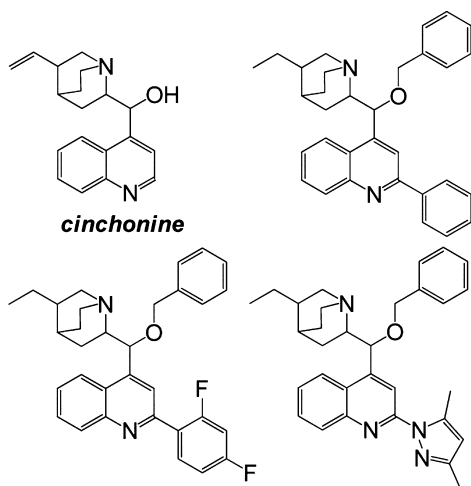
ABSTRACT: Ir(III) complexes of cyclometalating ligands derived from the natural product cinchonine and bent (4,6-bis(diphenylphosphino)phenoxazine (Nixantphos), 4,5-bis(diphenylphosphino)-9,9-dimethylxanthene (Xantphos)) and planar diphosphine ligands (1,2-bis(diphenylphosphino)benzene (dppb)) exhibit good luminescence with quantum efficiencies higher than those of their parent congeners. Steric hindrance by both the bulky cinchonine-derived ligand and bent diphosphine could limit nonradiative energy transfer. The cinchonine-derived and parent complexes cover a broad emission range from 472 to 569 nm with quantum efficiencies up to 0.38 and lifetimes from 0.01 to 0.46 μ s in degassed CH₂Cl₂ solution at room temperature. DFT calculations on selected examples are in good agreement with solid-state structures determined crystallographically and accurately predict wavelengths of emission by excited electron decay from a quinoline-centered orbital to an Ir 5d–phenyl molecular orbital. The complex [(pcn)₂Ir(Nixantphos)][PF₆] (**2**; pcn = 2'-phenyl-9-O-benzyl-10,11-dihydrocinchonine-C₂N) exhibits the highest quantum yield and could detect electron-deficient aromatic species at ppm levels.



INTRODUCTION

We have recently reported that, with relatively straightforward synthetic modifications, *Cinchona* alkaloid derivatives (Chart 1) function as novel cyclometalating and coordinating ligands for phosphorescent Ir(III) complexes.^{1,2} The bulky 1-

Chart 1

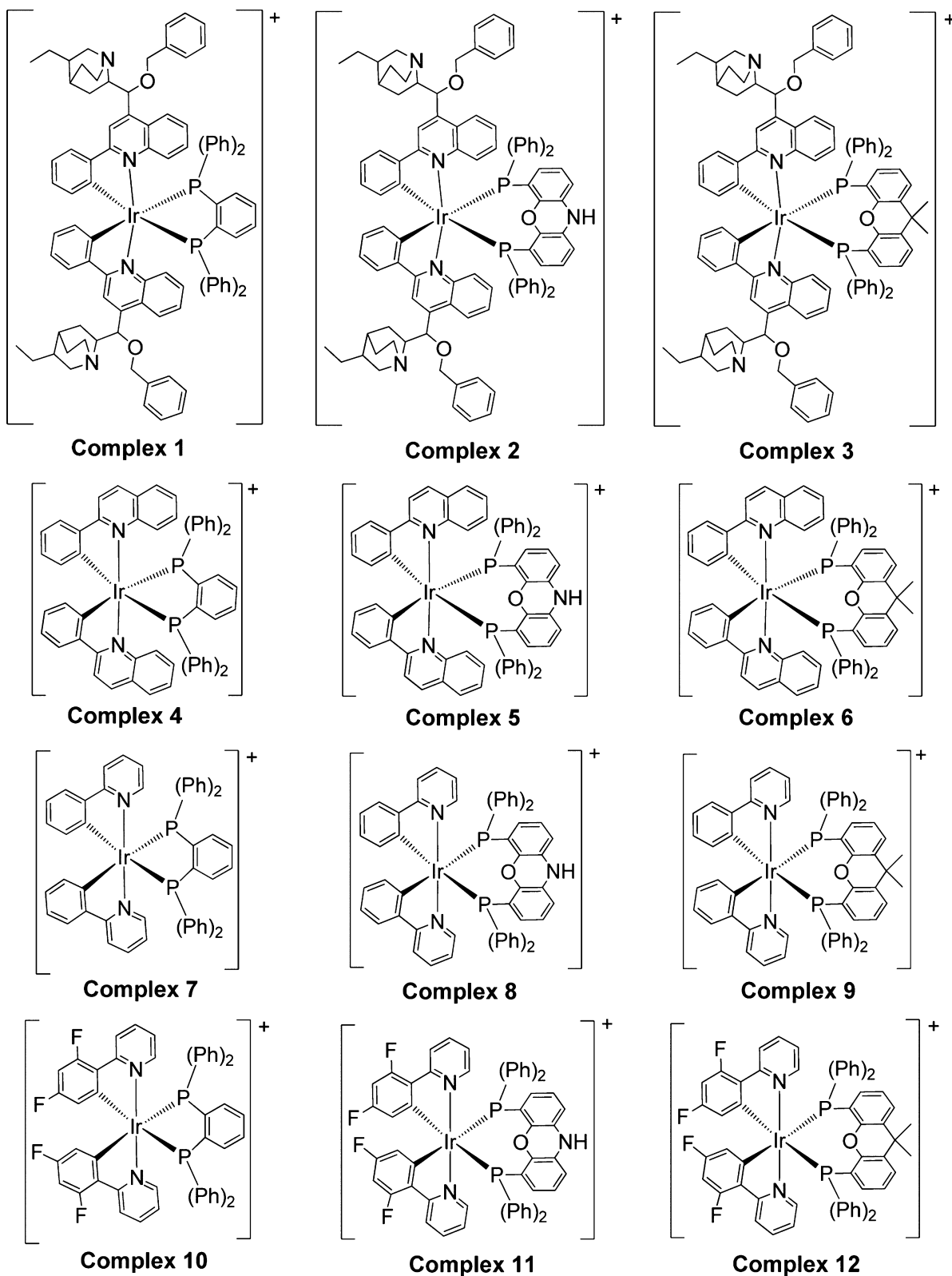


azabicyclo[2.2.2]octane and benzyl moieties improve solubility and serve to protect emission from triplet–triplet annihilation.^{3–6} As a result, these complexes are highly soluble in organic solvents and phosphoresce at tunable emission wavelengths by modifying cyclometalating or ancillary ligands. Improved quantum efficiencies of these complexes were observed in comparison to those of their quinoline congeners.^{7,8} In view of the increasingly diverse applications of these second and third row transition metal based phosphors in organic light-emitting diodes (OLEDs),^{9–30} light-emitting electrochemical cells (LECs),^{31–37} sensing,^{38–44} biological labeling and imaging,^{45–48} photoredox catalysts,^{49–53} and metal–organic frameworks,^{44,54–56} further improvement in the emission efficiency of these *Cinchona* alkaloid based Ir(III) complexes is worthy of investigation.

To obtain highly emissive Ir(III) complexes, we incorporated the bent-diphosphine ligands 4,6-bis(diphenylphosphino)-phenoxazine (Nixantphos) and 4,5-bis(diphenylphosphino)-9,9-dimethylxanthene (Xantphos), which are commonly found as ligands in transition-metal-based catalysis^{57–62} but are exotic as chelators in luminescent materials.⁶³ We proposed that the bent-diphosphine backbones would serve to reduce non-

Received: January 13, 2013

Published: May 13, 2013

Chart 2. Structures of Complexes 1–12^a

^aThe PF_6^- anions are omitted for clarity.

radiative relaxation of the excited cyclometalated complex by further hindering intermolecular stacking. In addition, the two methyl groups in Xantphos would provide further steric hindrance to intermolecular interactions. We surmised that

these features in tandem with the dendrimer-like cinchonine-derived ligand would maximize emission. To gauge the importance of each of these influences, we included the corresponding 2-phenylpyridine and 2-phenylquinoline cyclo-

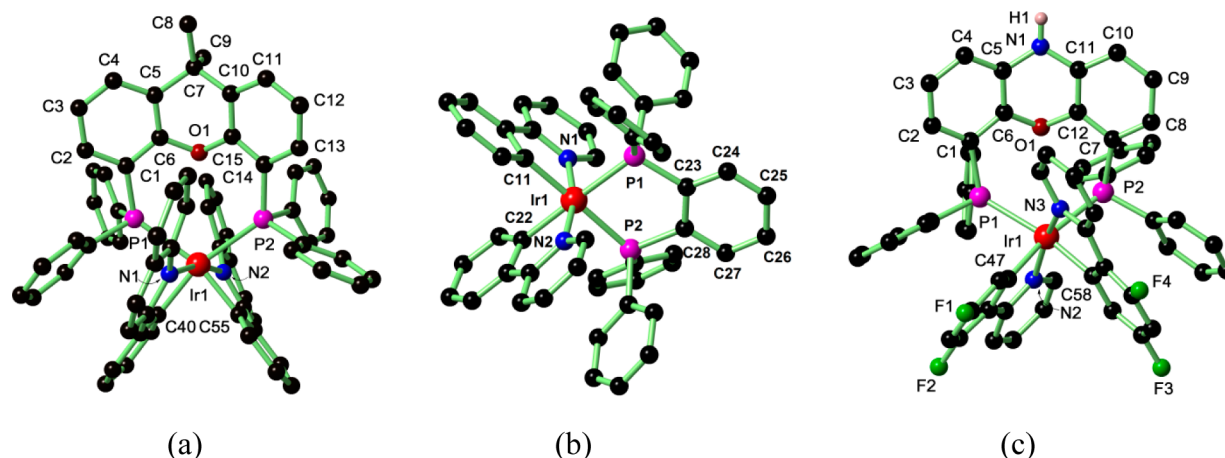


Figure 1. Complexes **6** (a), **7** (b), and **11** (c) with labeling scheme. Counterions, solvates, and hydrogen atoms, except H1 in **11**, are omitted for clarity.

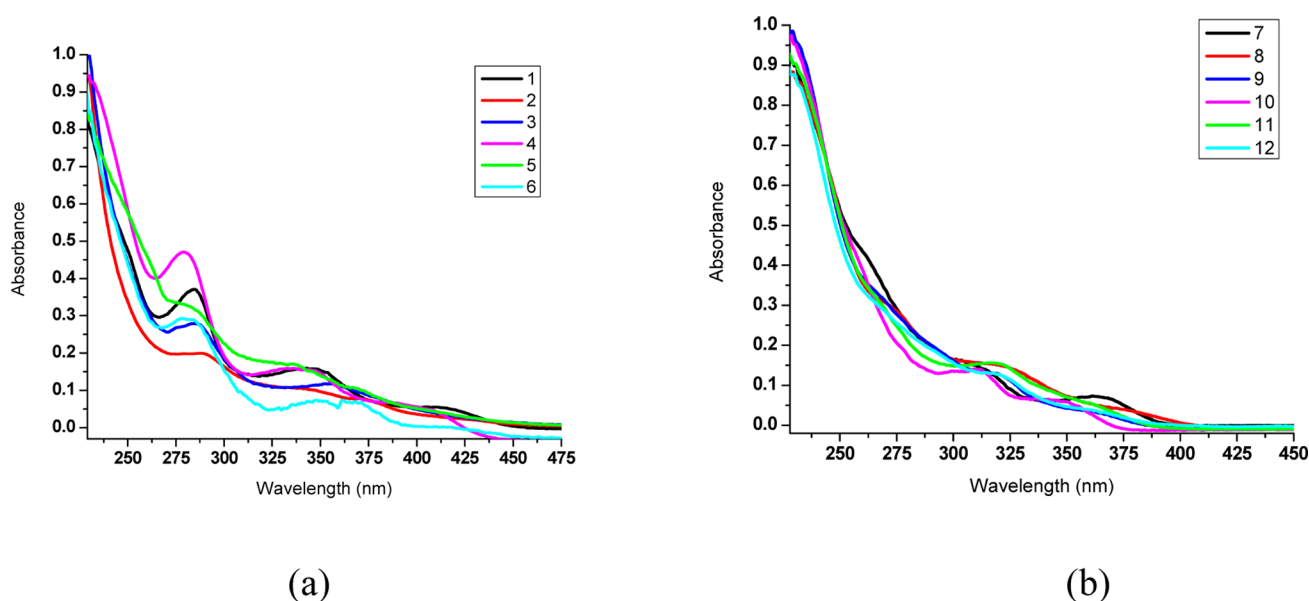


Figure 2. UV-vis spectra of complexes **1–6** (a) and **7–12** (b) recorded in degassed CH_2Cl_2 solutions at room temperature.

metalating complexes and 1,2-bis(diphenylphosphino)benzene (dppb) auxiliary ligand with a planar benzene backbone. The dinuclear Ir(III) complexes $[(\text{pcn})_2\text{IrCl}]_2$ (**P1**), $[(\text{pq})_2\text{IrCl}]_2$ (**P2**), $[(\text{ppy})_2\text{IrCl}]_2$ (**P3**), and $[(\text{fppy})_2\text{IrCl}]_2$ (**P4**) (pcn = 2'-phenyl-9-O-benzyl-10,11-dihydrocinchonine- C_2N ; pq = 2-phenylquinolinato- C_2N ; ppy = 2-phenylpyridinato- C_2N ; fppy = 2-(4,6-difluorophenyl)pyridinato- C_2N) were combined with our three diphosphine ligands to yield an array of 12 cationic, mononuclear Ir(III) species (Chart 2). The energy of relevant molecular orbitals in $[(\text{pq})_2\text{Ir}(\text{Xantphos})][\text{PF}_6]$ (**6**) was calculated using DFT methods to provide insight into the mechanism of emission. The high quantum efficiency of 0.38 for $[(\text{pcn})_2\text{Ir}(\text{Nixantphos})][\text{PF}_6]$ (**2**) permitted a preliminary study of its use as a chemical sensor for detection of the electron-deficient species 1-fluoro-4-nitrobenzene, 1-bromo-2,4-dinitrobenzene, and 4-nitrophthalonitrile at ppm levels.

RESULTS AND DISCUSSION

Synthesis of 1–12 and X-ray Structures of 6–8, 10, and 11. The syntheses of complexes **1–12** were similar and employed established procedures.^{1,2,32,64} The dinuclear iridium-

(III) precursors (**P1–P4**) were refluxed with diphosphine ligands in $\text{CH}_2\text{Cl}_2/\text{MeOH}$ (2/1, v/v) followed by an anion exchange using excess NH_4PF_6 and column separation to give orange, orange-red, or yellow-green fine powders. These complexes show good solubility in CH_2Cl_2 , CHCl_3 , MeCN, and DMSO. Complexes **1–12** were characterized by ^1H , ^{13}C , and ^{31}P NMR spectroscopy and ESI-MS spectrometry and additional ^{19}F NMR analysis for **10–12**. The ESI-MS spectra gave diagnostic peaks which are ascribed to $[(\text{C}^{\wedge}\text{N})_2\text{Ir}(\text{P–P})]^+$ ($\text{C}^{\wedge}\text{N}$ delineates cyclometalating ligands and P–P delineates diphosphine ligands; see the Experimental Section). The ^{31}P NMR spectra for these complexes are also diagnostic and the singlet resonances from -30.2 to 21.9 ppm indicated chemical equivalence for the two phosphorus atoms, whereas the septets at around -145 ppm are characteristic of PF_6^- anions. Complexes **1–12** were further characterized by FT-IR and their bulk purity confirmed by elemental analysis.

Single-crystal structures of **6–8**, **10**, and **11** were obtained through X-ray diffraction studies. These complexes exhibit some common structural characteristics: the Ir(III) center adopts a distorted-octahedral geometry with the two N donor

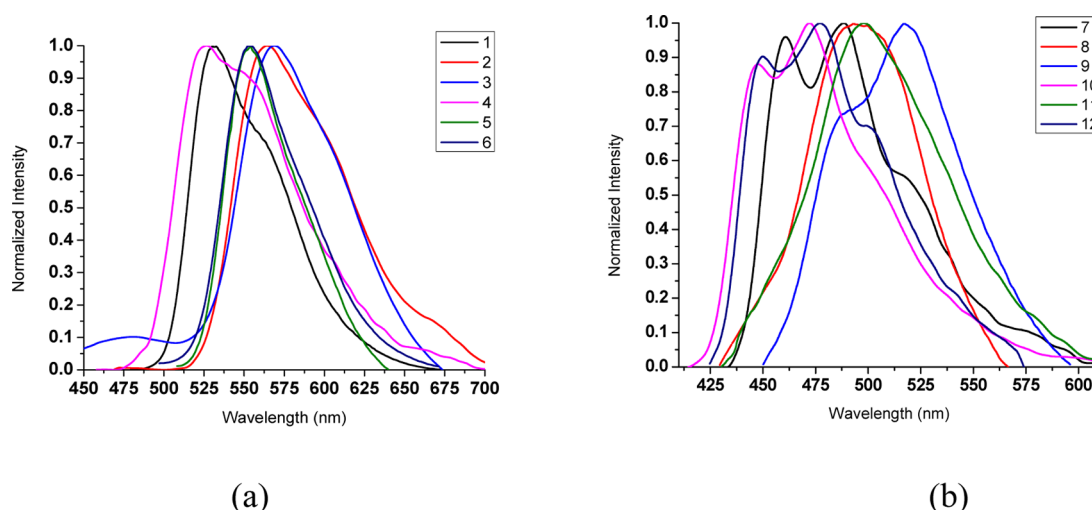


Figure 3. Normalized luminescence spectra of complexes 1–6 (a) and 7–12 (b) recorded in degassed CH_2Cl_2 solutions at room temperature.

Table 1. Photophysical Data for 1–12 in Degassed CH_2Cl_2 at Room Temperature

complex	UV–vis, nm (ϵ , $10^3 \text{ L mol}^{-1} \text{ cm}^{-1}$)	emission λ_{max} , nm	Φ^a	τ , μs
$[(\text{pcn})_2\text{Ir}(\text{dppb})][\text{PF}_6]$ (1)	227 (59.9), 284 (26.1), 344 (11.1), 414 (3.7)	531	0.19	0.13, 0.01
$[(\text{pcn})_2\text{Ir}(\text{Nixantphos})][\text{PF}_6]$ (2)	229 (154.6), 289 (32.6), 344 (16.7), 373 (12.5), 427 (3.6)	563	0.38	0.03, 0.10
$[(\text{pcn})_2\text{Ir}(\text{Xantphos})][\text{PF}_6]$ (3)	228 (126.5), 285 (32.7), 356 (13.8), 482 (0.8)	569	0.16	0.01, 0.40
$[(\text{pq})_2\text{Ir}(\text{dppb})][\text{PF}_6]$ (4)	230 (51.6), 280 (25.6), 334 (8.6), 345 (8.4), 385 (3.7), 406 (2.7)	525	0.047	0.09, 0.006
$[(\text{pq})_2\text{Ir}(\text{Nixantphos})][\text{PF}_6]$ (5)	227 (43.8), 274 (14.0), 338 (8.0), 435 (0.8)	553	0.048	0.01, 0.002
$[(\text{pq})_2\text{Ir}(\text{Xantphos})][\text{PF}_6]$ (6)	227 (39.0), 282 (12.1), 349 (3.8), 362 (3.9), 410 (1.2)	555	0.025	0.46
$[(\text{ppy})_2\text{Ir}(\text{dppb})][\text{PF}_6]$ (7)	228 (74.0), 263 (33.6), 307 (12.6), 363 (5.9)	488	0.16	0.002, 0.08
$[(\text{ppy})_2\text{Ir}(\text{Nixantphos})][\text{PF}_6]$ (8)	228 (88.4), 270 (30.6), 310 (16.1), 373 (4.6)	495	N.A.	0.008, 0.015
$[(\text{ppy})_2\text{Ir}(\text{Xantphos})][\text{PF}_6]$ (9)	227 (68.5), 263 (24.4), 318 (9.4), 358 (3.1)	517	0.0010	0.004, 0.030
$[(\text{F}_2\text{ppy})_2\text{Ir}(\text{dppb})][\text{PF}_6]$ (10)	228 (68.5), 256 (31.6), 278 (14.1), 312 (10.7), 343 (5.3)	472	0.30	0.22, 0.02
$[(\text{F}_2\text{ppy})_2\text{Ir}(\text{Nixantphos})][\text{PF}_6]$ (11)	227 (68.2), 263 (22.7), 318 (8.5), 358 (3.0)	497	0.00070	0.003, 0.06
$[(\text{F}_2\text{ppy})_2\text{Ir}(\text{Xantphos})][\text{PF}_6]$ (12)	227 (65.7), 262 (23.9), 314 (9.6), 356 (3.0)	476	0.020	0.004, 0.06

^aWith respect to Rhodamine 6G ($\Phi = 0.95$ in ethanol).

atoms invariably *trans* to each other and the phosphine donors *trans* to the two Ir–C bonds, regardless of the steric demands of the phosphine and cyclometalating ligands (Figure 1, Figure S1 (Supporting Information)). The average Ir–P bond distance for 7 (2.35 Å, Table S4 (Supporting Information)) is much shorter than those found in 6 (2.57 Å) and 11 (2.51 Å), which is ascribed to the reduced bite angle (five-membered ring in 7 vs eight-membered rings in 6 and 11). It is nonetheless longer than those found in $[\text{Ir}(\text{tpitH})(\text{PPh}_3)_2\text{Cl}_2]$ (Ir–P_{tpitH} = 2.1898(12) Å) and doubly fused five-membered rings in $[\text{Ir}(\text{tpit})(\text{PPh}_3)_2\text{Cl}]$ (Ir–P_{tpit} = 2.1529(8) Å).⁶⁵ Furthermore, average Ir–P bond distances found in 6 and 11 are much longer than those found in $\text{Rh}(\text{Nixantphos})(\text{CO})\text{H}(\text{PPh}_3)$ (average 2.34 Å),⁶⁶ $\text{Ir}(\text{Nixantphos})\text{Cl}(\text{COD})$ (average 2.43 Å),⁵⁸ $\text{Ir}(\text{Xantphos})(\text{CO})_2\text{Cl}$ (average 2.42 Å), and $\text{Ir}(\text{Xantphos})(\text{CO})_2\text{Br}$ (average 2.41 Å),⁶⁷ probably due to the strong *trans* effect of the Ir–C bond, which serves to weaken the Ir–P bonds. The respective average Ir–C and Ir–N bond distances of 2.06 and 2.10 Å (6), 2.06 and 2.07 Å (7), and 2.03 and 2.06 Å (11) are similar and comparable to those in related cyclometalated iridium(III) complexes.^{7,8,68} The two phenyl rings in the Xantphos backbone of 6 are tilted with a dihedral angle between C1–C2–C3–C4–C5–C6 and C10–C11–C12–C13–C14–C15 of 31.0°. The two cyclometalated phenylquinoline rings are also distorted and deviate from coplanarity. Similar observations have been reported for other

cyclometalated phenylquinoline complexes.^{69–72} The two phenyl rings in the Nixantphos backbone of 11 are tilted with a dihedral angle between C1–C2–C3–C4–C5–C6 and C7–C8–C9–C10–C11–C12 of 29.8°, which is similar to the corresponding distortion in 6.

Photophysical Properties of 1–12. The UV–vis absorption and emission spectra of complexes 1–12 are given in Figures 2 and 3, and the details are given in Table 1.

The absorption spectra of all the complexes are dominated by multiple bands originating from ligand-centered π – π^* transitions and MLCT transitions, in common with many cyclometalated Ir(III) complexes. The intense bands in the UV–vis spectra for all complexes in the high-energy portion of the spectra between 230 and 350 nm can be assigned to the spin-allowed $^1(\pi$ – $\pi^*)$ ligand transition. The weaker, low-energy bands at wavelengths longer than 400 nm suggest substantial mixing of spin-forbidden $^3\text{MLCT}$ and higher-lying $^1\text{MLCT}$ transitions facilitated by the strong spin–orbit coupling of the Ir(III) center (Figure 2).^{8,10,68,73–75}

Complexes 1–12 give intensive emissions in a broad range of color from 472 nm for 10 (blue) to 569 nm for 3 (orange). The quantum yields for these complexes are up to 0.38 (2) at room temperature, and lifetimes are in the range 0.01–0.46 μs . Vibronic fine structures were observed for dppb- and Xantphos-based structures 1, 4, 7, 9, 10, and 12, indicating that the emission for these complexes is dominated by ligand-based

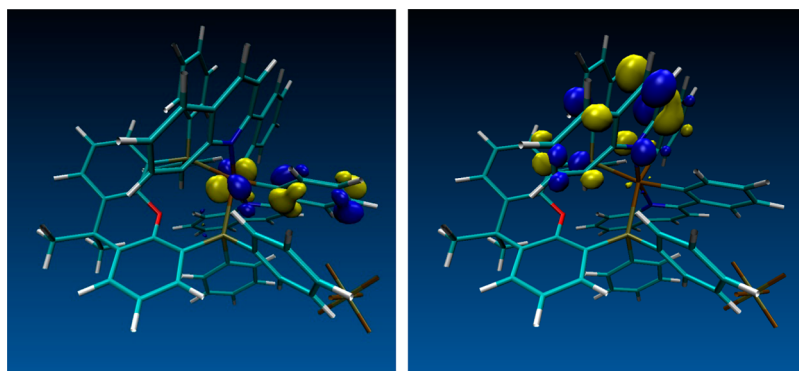


Figure 4. HOMO (left) and LUMO (right) energy orbitals of **6** through DFT calculations.

($^3\pi-\pi^*$) states. Meanwhile, the line shapes for the other complexes (**2**, **3**, **5**, **6**, **8**, and **11**) were structureless, suggesting emission primarily from MLCT states.^{8,68} It should be noted that the emission wavelengths for **2** (563 nm) and **3** (569 nm) are similar, suggesting that the excited triplet energies for Nixantphos and Xantphos are too high relative to 2-phenylquinoline and the emission is dominated by the [(pcn)₂Ir] moiety. This observation is further supported by the similar emission wavelengths of **5** (553 nm) and **6** (555 nm). This assumption is supported by the DFT calculations discussed below. Obvious blue shifts to 531 nm (**1**) and 525 nm (**4**) were observed for **1** and **4**, which both bear dppb as chelating ligand, indicating that their HOMO has significant diphosphine chelate character.⁷⁶ On comparison of **1–6**, **7–9**, and **10–12**, it can be surmised that both the reduced conjugation from quinoline to benzene and substitution of F for H in a chromophore (ppy to fppy) leads to a hypsochromic shift in emission.

Strong spin–orbit coupling leads to efficient phosphorescence in the majority of the complexes. The room-temperature quantum yields of these complexes in degassed CH₂Cl₂ were up to 0.38, and their luminescent lifetimes fall between 0.01 and 0.46 μ s, consistent with emission from a triplet excited state. Moreover, the steric hindrance by the bulky cinchonine ligand and bent-diphosphine ligand presumably prevents deactivation of the emitters by limiting energy transfer between the complexes. This is evidenced by the higher quantum efficiency of complexes **1–3** relative to the parent phenylquinoline complexes **4–6**. The quantum yield of 0.38 for **2** is higher than those for quinoline/isoquinoline derived emitters previously reported ((pq)₂Ir(acac), 0.10;^{7,8} Ir(piq)₃, 0.26⁷³) and our previously reported cinchonine complexes with nitrogen heterocyclic auxiliary ligands [(pcn)₂Ir(bipy)][PF₆] (0.23) and [(pcn)₂Ir(phen)][PF₆] (0.24).²

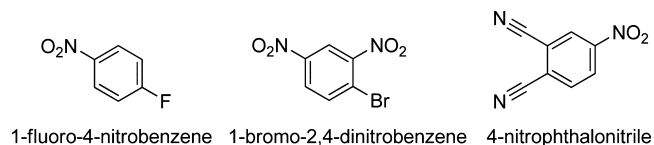
The Ir–P distances in dppb complexes **7** and **10** (2.3523(9)–2.3727(11) Å) are much shorter than those in Nixantphos and Xantphos complexes **6**, **8**, and **11** (2.4688(15)–2.5801(18) Å) (Table S4 (Supporting Information)). The shorter Ir–P bond means a stronger ligand field and further destabilization of the metal-centered d–d excited states, thereby favoring radiative decay. This could explain why dppb complexes **7** and **10** are more efficient emitters than their respective Nixantphos and Xantphos analogues.⁷⁷

DFT Calculations. In order to gain insight into the electronic structure of the complexes, we have carried out DFT calculations on nine selected complexes using the SIESTA package⁷⁸ with generalized gradient approximation at the GGA-PBE level and the optimized double- ζ plus polarization basis

set, as utilized in previous work.⁷⁹ The detailed orbital energy level as well as calculated bond distances and angles are given in Tables S1 and S2 (Supporting Information). These results suggest that Nixantphos- and Xantphos-based complexes have similar HOMO and LUMO surfaces and that phosphorescence is due to excited electron decay from a quinoline-dominated LUMO to the HOMO, which has significant metal 5d–phenyl π character. The average calculated bond distances for Ir–P (2.60 Å), Ir–C (2.05 Å), and Ir–N (2.12 Å) and chelate angles for P–Ir–P (109.8°), N–Ir–N (165.6°), and C–Ir–C (80.4°) in complex **6**, for example, compare favorably with the experimental values determined by X-ray single-crystal diffraction (Table S4 (Supporting Information)). The C–O–C–C torsion angle of 139.1° calculated for **6** is also similar to that found in the X-ray crystal structure (average 143.2°). The singlet HOMO and LUMO and triplet spin-density surfaces of [(pq)₂Ir(Xantphos)]⁺ are illustrated in Figure 4. The calculated HOMO and LUMO energies in the ground state are –5.15 and –3.35 eV, respectively. The HOMO is principally composed of a mixture of Ir d and phenyl π orbitals, whereas the LUMO is predominantly localized on the quinoline moiety of the cyclometalating ligands. The calculated MLCT gap of 2.26 eV (548 nm) is in good agreement with the energy of the emission band found for **6** (555 nm) in CH₂Cl₂ at room temperature.

Sensing. We proposed that complexes **1–3** which carry bulky cinchonine-derived ligands and electron-rich diphosphine moieties would interact strongly with electron-deficient aromatic compounds, resulting in a decrease in photoluminescent intensity of the complexes. To test this hypothesis, we selected 1-fluoro-4-nitrobenzene, 1-bromo-2,4-dinitrobenzene, and 4-nitrophthalonitrile as analytes (Chart 3).

Chart 3



Complex **2** was titrated with each analyte in degassed CH₂Cl₂ solution. Photoluminescence decreased to less than a third of its original value (Figures 5–9). This analyte-induced reduction is ascribed to the formation of an electron donor–acceptor pair between the Ir(III) complexes and the electron-deficient analytes; there is a charge transfer from the phosphor excited state to the low-lying molecular orbital associated with

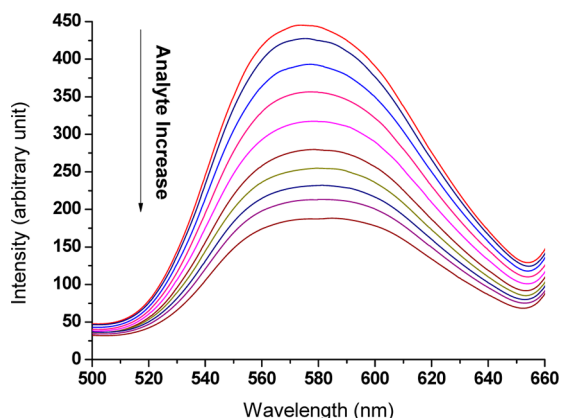


Figure 5. Titration of complex **2** with 1-fluoro-4-nitrobenzene in degassed CH_2Cl_2 at an excitation wavelength of 390 nm.

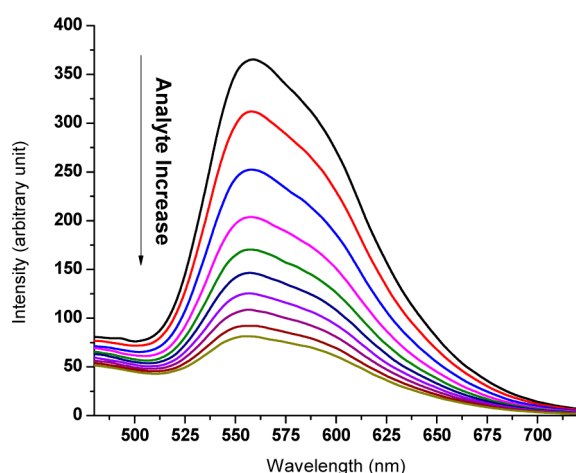


Figure 6. Titration of complex **2** with 4-nitrophthalonitrile in degassed CH_2Cl_2 at an excitation wavelength of 390 nm.

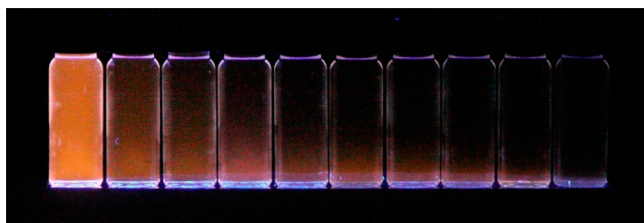


Figure 7. Fluorescence change on titration of complex **2** with 4-nitrophthalonitrile at an excitation wavelength of 365 nm with analyte concentration increasing from left to right.

the strongly electron-withdrawing nitro group.^{80,81} The probable location of contact between analyte and complex is at the ancillary diphosphine ligand because of the steric hindrance provided by the bulky quinuclidine moiety.

The detection limit of a 0.2 μM solution of complex **2** toward 1-fluoro-4-nitrobenzene under these conditions was between 3.6 and 9 ppm of analyte (see Figures 10 and 11).

Indeed, titration with 3.6 ppm analyte resulted in a slight increase in emission by the complex. This may be due to inhibition of aggregation by the photoluminescent complex.

CONCLUSION

A comparative study of cinchonine-derived cyclometalated Ir(III) diphosphines and their parent congeners indicates the

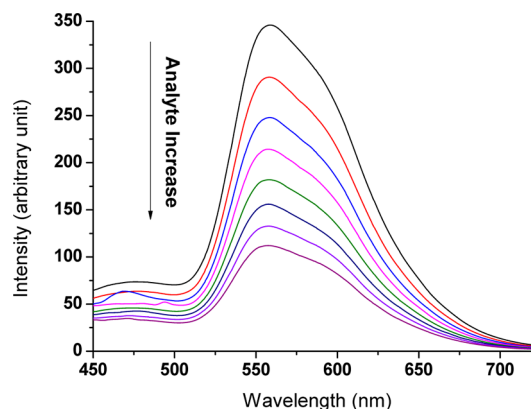


Figure 8. Titration of complex **2** with 1-bromo-2,4-dinitrobenzene in degassed CH_2Cl_2 at an excitation wavelength of 390 nm.

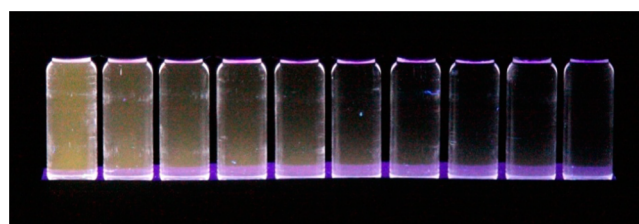


Figure 9. Fluorescence change on titration of complex **2** with 1-bromo-2,4-dinitrobenzene at an excitation wavelength of 365 nm with analyte concentration increasing from left to right.

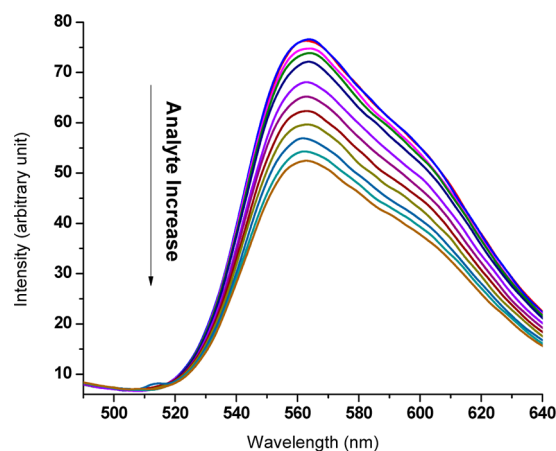


Figure 10. Titration of a $2.05 \times 10^{-7} \text{ mol L}^{-1}$ solution of complex **2** in degassed CH_2Cl_2 with a 9 ppm solution of 1-fluoro-4-nitrobenzene at an excitation wavelength of 345 nm.

superior emission properties of the former. This is enhanced by the bent chelating diphosphine ligands. The energy-harvesting ability, inherent chirality, and ligand hemilability of these natural product derived Ir(III) complexes suggest their potential as photoredox catalysts. Complex **2** is sensitive to electron-deficient aromatic species at ppm levels and hence may potentially be used for the detection of TNT and related explosives. We are exploring these possibilities.

EXPERIMENTAL SECTION

All synthetic procedures involving $\text{IrCl}_3 \cdot x\text{H}_2\text{O}$ and other Ir(III) species were carried out in the dark and under a N_2 atmosphere using standard Schlenk techniques. Elemental analyses were performed on a Perkin-Elmer PE 2400 CHNS Elemental Analyzer. The ^1H , ^{13}C , and ^{31}P

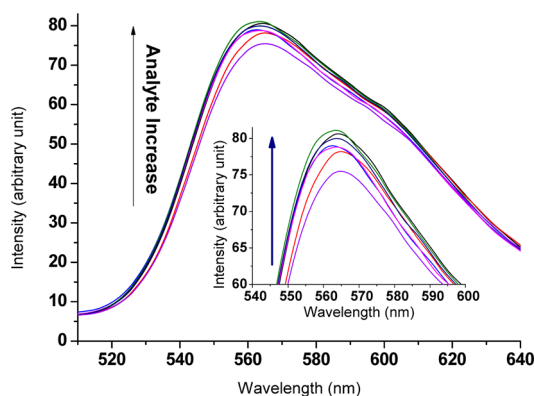


Figure 11. Titration of a 2.05×10^{-7} mol L $^{-1}$ solution of complex **2** with a 3.6 ppm solution of 1-fluoro-4-nitrobenzene in degassed CH $_2$ Cl $_2$ at an excitation wavelength of 345 nm.

NMR spectra were recorded on a Bruker AMX 400 MHz (Bruker AMX 500 MHz for complex **1**) spectrometer, and their chemical shifts were referenced to Me $_4$ Si (TMS) (1 H and 13 C) or 85% H $_3$ PO $_4$ (31 P). The 19 F NMR spectra were recorded on a Bruker ACF 300 spectrometer. IR spectra were recorded on a Bruker IFS 48 FTIR spectrometer as KBr pellets. UV-vis spectra were recorded on a UVIKON spectrometer. Electrospray mass spectra were obtained in positive-ion mode with a Finnigan/MAT LCQ mass spectrometer. Peaks were assigned from the m/z values and the isotope distribution patterns. Photoluminescence was measured using a Perkin-Elmer LS55 luminescence spectrometer and the quantum yield determined using Rhodamine 6G (quantum yield 0.95 in ethanol) as reference.⁸² The phosphorescence lifetime was measured using an Edinburgh FL920P Lifetime Spectrometer.

Synthesis of [(pcn) $_2$ Ir(dppb)][PF $_6$] (1**).** A mixture of [(pcn) $_2$ IrCl] $_2$ (**P1**; 0.23 g, 0.1 mmol) and 1,2-bis(diphenylphosphino)benzene (dppb; 0.094 g, 0.21 mmol) in a double-necked flask was flushed three times with N $_2$. A CH $_2$ Cl $_2$ /MeOH mixture (20 mL/10 mL) was added under N $_2$ and the solution heated to reflux for 12 h. The solution was then cooled to room temperature and NH $_4$ PF $_6$ (0.16 g, 1.0 mmol) in MeOH (5 mL) added under N $_2$. The mixture was stirred for another 15 h and the solvent evaporated. The resulting orange-red residue was dried under vacuum and CH $_2$ Cl $_2$ (5 mL) added. NH $_4$ Cl was removed by filtration. The solvent was removed and the product purified by chromatography on neutral Al $_2$ O $_3$ column using ethyl acetate/MeOH (30/1 v/v) as eluent to give an orange-red solid. Yield: 0.28 g (82% based on Ir). 1 H NMR (500 MHz, CD $_2$ Cl $_2$): δ 8.62–8.66 (m, 2H), 8.24–8.27 (m, 2H), 8.02 (s, 1H), 7.83–7.85 (m, 1H), 7.75–7.77 (m, 1H), 7.67–7.68 (m, 1H), 7.51–7.62 (m, 4H), 7.33–7.44 (m, 9H), 7.24–7.29 (m, 2H), 7.12–7.17 (m, 5H), 6.78–6.84 (m, 1H), 6.53–6.62 (m, 2H), 6.45–6.49 (m, 3H), 6.34–6.40 (m, 4H), 5.01–5.73 (m, 4H), 4.34–4.39 (m, 2H), 2.91–2.95 (m, 2H), 2.69–2.81 (m, 6H), 1.83–2.05 (m, 2H), 1.68–1.74 (m, 1H), 1.22–1.52 (m, 7H), 0.85–0.88 (m, 3H) ppm. 13 C{ 1 H} NMR (126 MHz, CD $_2$ Cl $_2$): δ 171.1, 168.9, 152.1, 151.3, 147.4, 147.4, 145.3, 145.0, 139.8, 139.6, 139.5, 138.3, 137.9, 137.8, 134.2, 134.1, 133.9, 133.8, 133.6, 133.4, 133.9, 133.8, 133.6, 133.4, 133.0, 132.7, 132.5, 131.3, 131.2, 130.8, 129.1, 129.0, 128.9, 128.8, 128.7, 128.6, 128.5, 128.4, 128.3, 128.1, 127.2, 127.1, 126.9, 126.8, 126.7, 126.6, 126.5, 126.4, 124.3, 124.0, 72.1, 71.9, 62.0, 61.0, 51.3, 50.9, 50.5, 50.3, 37.8, 37.8, 28.0, 27.6, 26.8, 26.7, 25.6, 25.5, 12.1, 12.0 ppm. 31 P NMR (202 MHz, CD $_2$ Cl $_2$): δ 14.5, –143.6 (hept) ppm. MS (ESI) (CH $_2$ Cl $_2$, 150 $^\circ$ C): m/z 1561.6 [Ir(pcn) $_2$ (dppb)] $^+$, 781.6 [Ir(pcn) $_2$ (dppb) + H] $^{2+}$. Anal. Calcd for C $_{94}$ H $_{90}$ F $_6$ IrN $_4$ O $_2$ P $_3$: C, 66.12; H, 5.28; N, 3.28. Found: C, 66.50; H, 5.39; N, 3.39. IR (KBr pellet): 3422 (w), 3054 (w), 2930 (m), 2868 (m), 2349 (w), 1735 (w), 1655 (w), 1606 (m), 1579 (w), 1542 (m), 1455 (m), 1343 (m), 1370 (w), 1291 (w), 1202 (w), 1162 (w), 1110 (w), 1086 (m), 940 (w), 840 (s), 751 (m), 734 (m), 733 (m), 700 (m), 663 (w), 650 (w), 557 (m), 527 (m) cm $^{-1}$.

Synthesis of [(pcn) $_2$ Ir(Nixantphos)][PF $_6$] (2**).** Complex **2** was purified on a neutral Al $_2$ O $_3$ column using ethyl acetate/MeOH (30/1 v/v) as eluent to give an orange-red solid. Yield: 0.24 g (66% based on Ir). 1 H NMR (400 MHz, CDCl $_3$): δ 9.53–9.59 (m, 2H), 8.75–8.79 (m, 1H), 7.83 (br, 3H), 7.51–7.55 (m, 3H), 7.36–7.47 (m, 1H), 7.31–7.33 (m, 1H), 7.23–7.31 (m, 1H), 7.07–7.13 (m, 1H), 6.95–6.99 (m, 1H), 6.80–6.84 (m, 1H), 6.59–6.73 (m, 3H), 6.52–6.56 (m, 1H), 6.24–6.32 (m, 2H), 6.06–6.08 (m, 1H), 5.94–5.98 (m, 1H), 5.45–5.54 (m, 1H), 4.51–4.61 (m, 1H), 2.83–3.28 (m, 3H), 1.83–2.01 (m, 1H), 1.36–1.64 (m, 4H), 1.22–1.27 (m, 1H), 0.82–0.91 (m, 2H) ppm. 13 C{ 1 H} NMR (101 MHz, CDCl $_3$): δ 170.5, 148.6, 147.7, 146.7, 146.7, 137.7, 136.6, 133.7, 132.9, 132.9, 132.7, 132.1, 130.3, 129.9, 129.2, 128.9, 128.8, 128.7, 128.4, 128.3, 128.2, 127.9, 126.4, 126.0, 125.9, 123.2, 123.0, 118.8, 118.7, 72.2, 62.9, 62.8, 61.4, 60.8, 51.4, 51.0, 50.7, 50.6, 37.5, 27.7, 27.6, 27.4, 26.6, 26.5, 25.8, 25.7, 14.6, 12.3 ppm. 31 P NMR (162 MHz, CDCl $_3$): δ –30.2, –30.6 (sh), –143.0 (hept) ppm. MS (ESI) (CH $_2$ Cl $_2$, 150 $^\circ$ C): m/z 1666.3 [Ir(pcn) $_2$ (Nixantphos)] $^+$. Anal. Calcd for C $_{100}$ H $_{93}$ F $_6$ IrN $_5$ O $_3$ P $_3$: C, 66.23; H, 5.13; N, 3.86. Found: C, 66.01; H, 5.47; N, 3.73. IR (KBr pellet): 3390 (m), 3059 (w), 2926 (s), 2856 (m), 2346 (w), 1725 (w), 1602 (m), 1578 (m), 1543 (m), 1519 (w), 1455 (s), 1435 (m), 1406 (s), 1376 (m), 1294 (w), 1200 (m), 1160 (w), 1116 (m), 1091 (m), 1013 (m), 940 (w), 843 (s), 766 (w), 743 (m), 695 (m), 557 (m), 525 (m) cm $^{-1}$.

Synthesis of [(pcn) $_2$ Ir(Xantphos)][PF $_6$] (3**).** Complex **3** was purified on a neutral Al $_2$ O $_3$ column using ethyl acetate/MeOH (30/1 v/v) as eluent to give an orange-red solid. Yield: 0.21 g (55% based on Ir). 1 H NMR (400 MHz, CDCl $_3$): δ 9.48 (dd, J = 12.6, 8.7 Hz, 1H), 7.89 (dd, J = 11.9, 6.2 Hz, 2H), 7.51–7.29 (m, 5H), 7.23–7.08 (m, 3H), 7.05–6.93 (m, 1H), 6.81–6.50 (m, 7H), 6.41–6.22 (m, 3H), 6.16 (t, J = 7.6 Hz, 1H), 6.00 (t, J = 7.7 Hz, 2H), 5.65–5.37 (m, 1H), 4.65–4.54 (m, 1H), 4.51 (s, 1H), 3.11 (d, J = 6.5 Hz, 1H), 3.00–2.74 (m, 4H), 2.13–1.98 (m, 4H), 1.88 (dd, J = 26.8, 17.4 Hz, 2H), 1.72–1.35 (m, 6H), 1.32–1.20 (m, 1H), 0.91 (t, J = 7.1 Hz, 3H) ppm. 13 C{ 1 H} NMR (101 MHz, D $_2$ O): δ 170.76, 170.58, 156.93, 152.21, 151.95, 150.75, 148.91, 148.78, 146.79, 137.73, 135.53, 134.86, 133.59, 132.90, 132.69, 132.51, 132.43, 132.07, 130.16, 129.48, 129.15, 129.09, 128.71, 128.57, 128.40, 128.33, 128.05, 127.78, 126.46, 126.21, 125.97, 123.60, 123.38, 123.21, 119.46, 119.34, 72.18, 71.98, 63.20, 61.45, 51.48, 50.75, 37.83, 37.71, 37.42, 28.26, 27.63, 26.54, 26.44, 25.88, 25.68, 12.35 ppm. 31 P NMR (162 MHz, CD $_2$ Cl $_2$): δ –29.4, –145.0 (hept) ppm. MS (ESI) (CH $_2$ Cl $_2$, 150 $^\circ$ C): m/z 1693.3 [Ir(pcn) $_2$ (Xantphos)] $^+$. Anal. Calcd for C $_{103}$ H $_{98}$ F $_6$ IrN $_4$ O $_3$ P $_3$: C, 67.21; H, 5.33; N, 3.05. Found: C, 67.57; H, 5.42; N, 2.80. IR (KBr pellet): 3345 (m), 3056 (m), 2931 (s), 2868 (m), 1602 (s), 1580 (m), 1543 (m), 1517 (w), 1483 (m), 1453 (m), 1436 (m), 1407 (s), 1369 (m), 1291 (w), 1222 (m), 1201 (m), 1161 (w), 1116 (m), 1090 (m), 1027 (m), 999 (w), 940 (w), 842 (s), 790 (m), 747 (s), 695 (s), 650 (w), 610 (w), 557 (s), 520 (m), 531 (m) cm $^{-1}$.

Synthesis of [(pq) $_2$ Ir(dppb)][PF $_6$] (4**).** Complex **4** was purified on a silica gel column using ethyl acetate/MeOH (30/1 v/v) as eluent to give an orange-red solid. Yield: 0.090 g (38% based on Ir). 1 H NMR (400 MHz, CDCl $_3$): δ 8.47–8.51 (m, 1H), 8.14–8.16 (m, 1H), 7.95–7.97 (m, 1H), 7.81–7.83 (m, 1H), 7.72–7.74 (m, 1H), 7.42–7.51 (m, 5H), 7.33–7.36 (m, 2H), 7.21–7.26 (m, 2H), 7.04–7.15 (m, 5H), 6.77–6.81 (m, 1H), 6.58–6.61 (m, 1H), 6.28–6.36 (m, 5H), 5.74–5.77 (m, 1H) ppm. 13 C{ 1 H} NMR (101.1 MHz, CDCl $_3$): δ 172.0, 170.3, 147.1, 145.6, 140.3, 139.3, 134.1, 134.0, 133.5, 133.2, 132.1, 132.0, 131.9, 131.4, 131.1, 131.1, 130.9, 129.6, 129.4, 129.1, 128.8, 128.8, 128.7, 127.9, 127.3, 126.9, 126.8, 124.4, 118.8 ppm. 31 P NMR (162 MHz, CDCl $_3$): δ 14.1, –143.5 (hept) ppm. MS (ESI) (CH $_2$ Cl $_2$, 150 $^\circ$ C): m/z 1047.1 [Ir(pq) $_2$ (dppb)] $^+$. Anal. Calcd for C $_{60}$ H $_{44}$ F $_6$ IrN $_2$ P $_3$: C, 60.45; H, 3.72; N, 2.35. Found: C, 56.91; H, 3.64; N, 1.94 (corresponding to 4-CH $_2$ Cl $_2$). IR (KBr pellet): 3431 (w), 3050 (w), 2919 (m), 2850 (m), 1704 (w), 1606 (m), 1578 (m), 1547 (m), 1515, 1483 (w), 1453 (m), 1434 (m), 1330 (m), 1288 (w), 1265 (w), 1218 (w), 1147 (w), 1118 (w), 1089 (m), 1027 (w), 1000 (w), 841 (s), 790, 766 (s), 751 (m), 731 (m), 700 (m), 557 (s), 533 (s), 514 (m) cm $^{-1}$.

Synthesis of [(pq)₂Ir(Nixantphos)][PF₆] (5). Complex 5 was purified on a silica gel column using ethyl acetate/MeOH (30/1 v/v) as eluent to give an orange-red solid. Yield: 0.068 g (52% based on Ir). ¹H NMR (400 MHz, CDCl₃): δ 9.45–9.49 (m, 1H), 8.11–8.15 (m, 1H), 7.66–7.70 (m, 1H), 7.49–7.58 (m, 3H), 6.95–7.40 (m, 16H), 6.54–6.84 (m, 14H), 6.38–6.42 (m, 2H), 6.22–6.26 (m, 2H), 5.96–5.98 (m, 3H), 5.58–5.60 (m, 1H) ppm. ¹³C{¹H} NMR (101 MHz, CDCl₃): δ 162.1, 148.7, 146.5, 139.7, 136.0, 133.6, 132.7, 131.7, 130.6, 130.2, 130.0, 129.2, 129.0, 128.9, 128.8, 128.3, 128.2, 128.0, 126.5, 126.1, 125.9, 123.1, 118.4, 118.4, ppm. ³¹P NMR (162 MHz, CDCl₃): δ –30.4, –143.3 (hept) ppm. MS (ESI) (CH₂Cl₂, 150 °C): *m/z* 1152.0 [Ir(pq)₂(Nixantphos)]⁺. Anal. Calcd for C₆₆H₄₇F₆IrN₃OP₃: C, 61.06; H, 3.62; N, 3.24. Found: C, 61.00; H, 4.02; N, 2.67. IR (KBr pellet): 3338 (br), 3055 (m), 2927 (m), 2055 (m), 1610 (s), 1569 (s), 1518 (m), 1461 (s), 1438 (s), 1407 (s), 1295 (m), 1201 (m), 1117 (m), 1095 (m), 1028 (w), 999 (w), 872 (br), 728 (s), 693 (s), 557 (s), 518 (sh), 408 (w) cm^{–1}.

Synthesis of [(pq)₂Ir(Xantphos)][PF₆] (6). Complex 6 was purified on a silica gel column using ethyl acetate/MeOH (30/1 v/v) as eluent to give an orange-red solid. Yield: 0.127 g (46.9% based on Ir). ¹H NMR (400 MHz, CDCl₃): δ 9.40 (d, *J* = 8.6 Hz, 1H), 8.22 (d, *J* = 8.6 Hz, 1H), 7.86 (d, *J* = 7.5 Hz, 1H), 7.76 (d, *J* = 8.8 Hz, 1H), 7.61 (d, *J* = 7.8 Hz, 2H), 7.21–7.07 (m, 4H), 6.99 (t, *J* = 7.3 Hz, 1H), 6.74 (t, *J* = 7.3 Hz, 3H), 6.69–6.51 (m, 5H), 6.43 (t, *J* = 7.4 Hz, 2H), 6.25 (t, *J* = 7.3 Hz, 2H), 6.14 (t, *J* = 7.7 Hz, 1H), 5.92 (d, *J* = 7.1 Hz, 2H), 5.66 (d, *J* = 5.9 Hz, 1H), 2.02 (s, 3H) ppm. ¹³C{¹H} NMR (101 MHz, CDCl₃): δ 171.47, 156.85, 148.86, 146.59, 140.13, 135.34, 134.91, 133.56, 132.67, 131.90, 131.70, 130.38, 130.23, 129.58, 129.20, 128.59, 128.55, 128.14, 127.76, 127.19, 126.57, 126.15, 125.81, 123.33, 118.80, 37.32, 28.29 ppm. ³¹P NMR (162 MHz, CD₂Cl₂): δ –29.3, –145.0 (hept) ppm. MS (ESI) (CH₂Cl₂, 150 °C): *m/z* 1179.1 [Ir(pq)₂(Xantphos)]⁺. Anal. Calcd for C₆₉H₅₂F₆IrN₂OP₃: C, 62.54; H, 3.93; N, 2.11. Found: C, 61.34; H, 3.85; N, 2.05 (corresponding to [(pq)₂Ir(Xantphos)][PF₆]·0.3CH₂Cl₂). IR (KBr pellet): 3052 (m), 2963 (m), 2924 (m), 2858 (w), 2263 (w), 2025 (w), 1954 (w), 1819 (w), 1719 (w), 1685 (w), 1606 (s), 1578 (s), 1549 (s), 1517 (s), 1482 (m), 1465 (m), 1451 (m), 1438 (s), 1406 (s), 1364 (w), 1339 (m), 1291 (m), 1273 (w), 1241 (m), 1219 (s), 1197 (m), 1167 (m), 1148 (w), 1085 (m), 1038 (w), 1027 (m), 999 (m), 915 (m), 875 (s), 843 (s), 791 (s), 765 (s), 746 (s), 723 (s), 695 (s), 642 (m), 610 (w), 557 (s), 532 (m), 520 (s), 493 (m), 458 (s), 443 (w), 418 (w) cm^{–1}.

Synthesis of [(ppy)₂Ir(dppb)][PF₆] (7). Complex 7 was purified on a silica gel column using ethyl acetate/MeOH (30/1 v/v) as eluent to give a yellowish green solid. Yield: 0.13 g (57% based on Ir). ¹H NMR (400 MHz, CDCl₃): δ 8.07–8.11 (m, 2H), 7.97–7.98 (m, 2H), 7.58–7.62 (m, 4H), 7.42–7.53 (m, 12H), 7.31–7.32 (m, 2H), 7.02–7.06 (m, 2H), 6.96–7.00 (m, 2H), 6.89–6.93 (m, 2H), 6.76–6.79 (m, 4H), 6.27–6.35 (m, 6H), 6.14–6.16 (m, 2H), 5.29 (s, 1H) ppm. ¹³C{¹H} NMR (101 MHz, CDCl₃): δ 168.1, 158.3, 158.2, 157.4, 157.4, 152.9, 143.4, 141.2, 140.8, 140.4, 138.2, 137.5, 134.3, 134.3, 133.7, 132.0, 131.9, 130.9, 130.8, 130.7, 129.9, 129.7, 129.6, 129.1, 128.9, 128.7, 128.4, 125.3, 123.8, 123.2, 120.4 ppm. ³¹P NMR (162 MHz, CD₂Cl₂): δ 21.8, –143.7 (hept) ppm. MS (ESI) (CH₂Cl₂, 150 °C): *m/z* 947.2 [Ir(ppy)₂(dppb)]⁺. Anal. Calcd for C₅₂H₄₀F₆IrN₂P₃: C, 57.19; H, 3.67; N, 2.57. Found: C, 54.78; H, 3.52; N, 2.39 (corresponding to 7·CH₂Cl₂). IR (KBr pellet): 3671 (w), 3444 (m), 3125 (m), 3053 (m), 3003 (m), 2342 (w), 1982 (w), 1891 (w), 1821 (w), 1610 (s), 1582 (s), 1567 (m), 1554 (m), 1481 (s), 1454 (m), 1482 (m), 1454 (m), 1435 (s), 1318 (m), 1306 (m), 1271 (m), 1229 (m), 1188 (m), 1167 (m), 1111 (s), 1090 (s), 1067 (m), 1060 (m), 1050 (w), 1027 (m), 1000 (m), 947 (w), 928 (w), 910 (w), 852 (s), 780 (s), 753 (s), 699 (s), 665 (s), 630, 557 (s), 530 (s), 516 (s) cm^{–1}.

Synthesis of [(ppy)₂Ir(Nixantphos)][PF₆] (8). Complex 8 was purified on a silica gel column using ethyl acetate/MeOH (30/1 v/v) as eluent to give a yellowish green solid. Yield: 0.137 g (56% based on Ir). ¹H NMR (400 MHz, CDCl₃): δ 8.93 (s, 1H), 7.84 (br, 1H), 7.35–7.42 (m, 1H), 7.23–7.26 (m, 6H), 7.14 (br, 2H), 6.97–7.05 (m, 3H), 6.78–6.85 (m, 5H), 6.58–6.62 (m, 1H), 6.41–6.45 (m, 2H), 6.25–6.28 (m, 1H), 6.15 (s, 1H), 5.23–5.25 (m, 1H) ppm. ¹³C{¹H} NMR (101 MHz, CD₂Cl₂): δ 168.6, 155.7, 155.6, 155.5, 142.2, 140.2, 138.9,

135.1, 134.9, 134.8, 134.8, 132.8, 131.3, 130.4, 130.0, 129.8, 129.7, 129.6, 128.8, 128.7, 128.4, 126.0, 124.5, 124.4, 124.1, 123.1, 120.3 ppm. ³¹P NMR (162 MHz, CD₂Cl₂): δ –21.1, –143.4 (hept) ppm. MS (ESI) (CH₂Cl₂, 150 °C): *m/z* 1052.2 [Ir(ppy)₂(Nixantphos)]⁺. Anal. Calcd for C₅₈H₄₃F₆IrN₃OP₃: C, 58.15; H, 3.59; N, 3.51. Found: C, 57.85; H, 3.81; N, 3.23. IR (KBr pellet): 3392 (m), 3056 (w), 1608 (m), 1586 (m), 1571 (m), 1482 (s), 1456 (s), 1435 (s), 1398 (s), 1321 (w), 1295 (w), 1269 (w), 1228 (w), 1203 (w), 1168 (w), 1089 (w), 1027 (w), 999 (w), 845 (vs), 792 (w), 744 (s), 732 (s), 697 (s), 630 (w), 558 (s), 523 (s), 506 (m), 462 (w), 435 (w), 415 (w) cm^{–1}.

Synthesis of [(ppy)₂Ir(Xantphos)][PF₆] (9). Complex 9 was purified on a silica gel column using ethyl acetate/MeOH (30/1 v/v) as eluent to give a yellowish green solid. Yield: 0.20 g (89% based on Ir). ¹H NMR (400 MHz, CDCl₃): δ 8.61 (d, *J* = 5.7 Hz, 1H), 7.90 (q, *J* = 7.8 Hz, 2H), 7.57 (d, *J* = 7.6 Hz, 1H), 7.29–7.26 (m, 2H), 7.12–7.05 (m, 4H), 6.83 (d, *J* = 3.1 Hz, 4H), 6.76 (t, *J* = 6.7 Hz, 1H), 6.69 (t, *J* = 5.3 Hz, 1H), 6.60 (t, *J* = 7.4 Hz, 1H), 6.40 (t, *J* = 7.7 Hz, 2H), 6.24 (t, *J* = 7.4 Hz, 1H), 5.16 (d, *J* = 7.1 Hz, 1H), 1.49 (s, 3H) ppm. ¹³C{¹H} NMR (101 MHz, CDCl₃): δ 168.58, 154.64, 153.80, 153.34, 142.13, 139.31, 134.47, 133.02, 132.77, 131.47, 131.36, 131.02, 130.62, 130.29, 130.00, 129.93, 128.90, 128.42, 125.51, 124.58, 124.00, 123.27, 120.78, 118.89, 118.56, 118.23, 36.15, 29.02 ppm. ³¹P NMR (162 MHz, CD₂Cl₂): δ –20.2, –145.0 (hept) ppm. MS (ESI) (CH₂Cl₂, 150 °C): *m/z* 1079.1 [Ir(ppy)₂(Xantphos)]⁺. Anal. Calcd for C₆₁H₄₈F₆IrN₂OP₃: C, 59.80; H, 3.92; N, 2.29. Found: C, 58.69; H, 4.41; N, 1.97. IR (KBr pellet): 3855 (w), 3650 (w), 3421 (w), 3050 (w), 2961 (w), 1608 (m), 1583 (m), 1562 (m), 1480 (s), 1437 (m), 1409 (s), 1320 (w), 1232, 1167 (w), 1118 (w), 1027 (w), 1000 (w), 841, 792 (m), 750 (s), 734 (s), 696 (m), 630 (w), 609 (w), 587 (w), 557 (m), 534 (w) cm^{–1}.

Synthesis of [(Fppy)₂Ir(dppb)][PF₆] (10). Complex 10 was purified on a silica gel column using ethyl acetate/MeOH (30/1 v/v) as eluent to give a yellowish green solid. Yield: 0.044 g (36% based on Ir). ¹H NMR (400 MHz, CDCl₃): δ 8.06–8.13 (m, 2H), 7.85–7.87 (m, 1H), 7.48–7.61 (m, 6H), 7.37–7.39 (m, 1H), 7.07–7.11 (m, 1H), 6.83–6.86 (m, 2H), 6.51–6.56 (m, 1H), 6.35–6.43 (m, 3H), 5.56–5.59 (m, 1H) ppm. ¹³C{¹H} NMR (101 MHz, CDCl₃): δ 164.6, 162.4, 153.3, 139.0, 137.8, 134.5, 134.3, 134.2, 132.4, 131.0, 130.9, 130.0, 129.9, 128.7, 128.7, 127.8, 124.3, 124.1, 123.7, 114.1, 113.9, 100.3 ppm. ³¹P NMR (162 MHz, CDCl₃): δ 21.9, –143.8 (hept) ppm. ¹⁹F NMR (282 MHz, CDCl₃): δ 2.43 (d, *J*_{C–F} = 713 Hz), –29.68 to –29.74 (m), –31.70 to –31.72 (m), –77.97 (s) ppm. MS (ESI) (CH₂Cl₂, 150 °C): *m/z* 1019.3 [Ir(Fppy)₂(dppb)]⁺. Anal. Calcd for C₅₂H₃₆F₁₀IrN₂P₃: C, 53.66; H, 3.10; N, 2.41. Found: C, 52.85; H, 2.97; N, 2.37. IR (KBr pellet): 3855 (w), 3752 (w), 3650 (w), 3445 (w), 3136 (w), 3058 (w), 2924 (w), 2343 (w), 1631 (w), 1603 (s), 1578 (s), 1561 (m), 1481 (m), 1455 (w), 1434 (m), 1406 (m), 1295 (m), 1271 (w), 1252 (m), 1227 (w), 1191 (w), 1165 (m), 1109 (m), 1091 (m), 1040 (w), 991 (m), 844 (s), 783 (w), 740 (m), 753 (m), 702 (m), 668 (w), 617 (w), 569 (m), 558 (m), 541 (s), 532 (s) cm^{–1}.

Synthesis of [(Fppy)₂Ir(Nixantphos)][PF₆] (11). Complex 11 was purified on silica gel column using ethyl acetate/MeOH (30/1 v/v) as eluent to give a yellowish green solid. Yield: 0.23 g (89% based on Ir). ¹H NMR (400 MHz, CDCl₃): δ 8.69 (d, *J* = 5.6 Hz, 1H), 8.29–8.32 (m, 1H), 7.98–8.02 (m, 1H), 7.64 (d, *J* = 7.5 Hz, 1H), 7.38–7.41 (m, 1H), 7.13–7.23 (m, 4H), 6.81–6.95 (m, 6H), 6.61–6.68 (m, 1H), 6.44–6.48 (m, 2H), 6.10–6.16 (m, 1H), 4.56–4.58 (m, 1H) ppm. ¹³C{¹H} NMR (101 MHz, CDCl₃): δ 165.0 (m), 162.2 (m), 159.8 (m), 157.7 (m), 156.7 (m), 154.8, 153.7, 140.5, 134.3, 133.2, 132.6, 131.3, 130.7, 130.6, 130.0, 129.5, 129.2, 129.1, 128.6, 126.5, 125.9, 124.7, 124.5, 113.1, 112.9, 99.7 ppm. ³¹P NMR (162 MHz, CDCl₃): δ –23.8, –145.0 (hept) ppm. ¹⁹F NMR (282 MHz, CDCl₃): δ 2.39 (d, *J*_{C–F} = 712 Hz), –27.89 (s), –32.31 to –32.35 (m) ppm. MS (ESI) (CH₂Cl₂, 150 °C): *m/z* 1124.1 [Ir(Fppy)₂(Nixantphos)]⁺. Anal. Calcd for C₅₈H₃₉F₁₀IrN₃OP₃: C, 54.85; H, 3.07; N, 3.31. Found: C, 55.08; H, 3.33; N, 3.20. IR (KBr pellet): 3384 (m), 3141 (w), 3080 (m), 2925 (w), 2853 (w), 2613 (w), 2099 (w), 1969 (w), 1922 (w), 1846 (w), 1603 (s), 1577 (s), 1559 (s), 1522 (w), 1507 (w), 1480 (s), 1457 (s), 1434 (s), 1405 (s), 1297 (s), 1270 (m), 1254 (m), 1227 (m), 1207 (m), 1165 (s), 1110 (m), 1108 (s),

1089 (m), 1040 (w), 1027 (w), 993 (s), 842 (s), 786 (s), 741 (s), 696 (s), 663 (w), 569 (m), 557 (s), 525 (s), 503 (m), 461 (w), 448 (w), 435 (w) cm^{-1} .

Synthesis of $[(\text{Fppy})_2\text{Ir}(\text{Xantphos})][\text{PF}_6]$ (12). Complex 12 was purified on a silica gel column using ethyl acetate/MeOH (30/1 v/v) as eluent to give a yellowish green solid. Yield: 0.17 g (66% based on Ir). ^1H NMR (400 MHz, CDCl_3): δ 8.68–8.69 (m, 1H), 8.30–8.32 (m, 1H), 7.98–8.01 (m, 1H), 7.63–7.64 (m, 1H), 7.37–7.41 (m, 1H), 7.15–7.25 (m, 4H), 6.80–6.95 (m, 5H), 6.46–6.48 (m, 2H), 6.11–6.16 (m, 1H), 4.56–4.58 (m, 1H), 1.50 (s, 2H) ppm. ^{13}C $\{^1\text{H}\}$ NMR (101 MHz, CDCl_3): δ 164.87, 164.42, 162.12, 153.86, 153.50, 153.29, 148.12, 138.63, 136.28, 135.18, 134.42, 134.32, 134.22, 133.98, 133.74, 133.55, 132.89, 132.71, 132.48, 131.33, 130.42, 128.70, 128.52, 128.36, 128.25, 128.16, 128.00, 127.86, 127.11, 127.00, 126.71, 124.54, 124.38, 123.96, 123.72, 122.81, 122.69, 122.30, 121.82, 117.68, 117.49, 99.26, 97.01, 60.79, 58.60, 53.81, 34.78, 32.22, 30.09 ppm. ^{31}P NMR (162 MHz, CD_2Cl_2): δ -20.1, -143.7 (hept) ppm. ^{19}F NMR (282 MHz, CDCl_3): δ 2.36 (d, $J_{\text{C-F}}$ = 712 Hz), -27.81 to -27.87 (m), -32.28 to -32.35 (m) ppm. MS (ESI) (CH_2Cl_2 , 150 $^\circ\text{C}$): m/z 1151.2 $[\text{Ir}(\text{fppy})_2(\text{Xantphos})]^+$. Anal. Calcd for $\text{C}_{61}\text{H}_{44}\text{F}_{10}\text{IrN}_2\text{OP}_3$: C, 56.48; H, 3.40; N, 2.16. Found: C, 56.36; H, 3.70; N, 2.13. IR (KBr pellet): 3855 (w), 3737 (w), 3650 (w), 3400 (m), 3065 (m), 2971 (m), 2344 (w), 1971 (w), 1763 (w), 1602 (s), 1578 (s), 1480 (s), 1455 (m), 1434 (s), 1408 (s), 1366 (m), 1297 (m), 1270 (m), 1253 (s), 1197 (m), 1165 (m), 1119 (m), 1108, 1089 (m), 1040 (w), 1013 (w), 992 (s), 930 (w), 843 (s), 789 (m), 775 (m), 750 (s), 697 (s), 608 (w), 587 (w), 570 (m), 557 (m), 519 (s) cm^{-1} .

X-ray Crystallography for 6–8, 10, and 11. Crystallographic measurements were made on a Bruker AXS APEX diffractometer by using graphite-monochromated Mo $K\alpha$ (λ = 0.71073 Å). The data were corrected for Lorentz and polarization effects with the SMART suite of programs and for absorption effects with SADABS.⁸³ All crystal structures were solved by direct methods and refined on F^2 by full-matrix least-squares techniques with the SHELXTL-97 program.⁸⁴ The occupancy factors in 6, for all the free H_2O molecules, were fixed at 0.50 and refined isotropically to obtain satisfactory thermal parameters for these oxygen atoms, and the hydrogen atoms on these free H_2O molecules could not be found from a difference Fourier map. Both $[\text{PF}_6]^-$ anions in 7 adopt positional disorder, and the occupancy factors for all the disordered atoms were fixed at 0.50. CH_2Cl_2 solvent was also disordered with occupancy factors for C and Cl atoms fixed at 0.50. The hydrogen atoms on the free H_2O molecule could not be located from a difference Fourier map. In 8, the CH_2Cl_2 solvent has high thermal motion and its occupancy factor was fixed at 0.50 and refined isotropically to obtain reasonable thermal factors. C35–C40 had large ellipsoids, and packing diagram/void space generation revealed that this is due to the close proximity of a phenyl to the disordered solvent, anion, and a small void space. In 10, the occupancy factors of two MeCN solvates were fixed at 0.5 and 0.25 and refined isotropically to give reasonable thermal factors. The hydrogen atoms on the methyl groups were not located. The thermal motions for the phenyl ring containing C29–C34 also had large ellipsoids for reasons similar to those described for complex 8. A summary of the key crystallographic data for 6–8, 10, and 11 are given in Table S3, and selected bond distances and angles are given in Table S4 (Supporting Information).

■ ASSOCIATED CONTENT

■ Supporting Information

Tables and figures files giving detailed DFT results, crystallographic data for 6–8, 10, and 11, selected bond distances and angles for 6–8, 10, and 11, X-ray structures of 8 and 10 with labeling, and ^1H , ^{13}C , ^{31}P , and ^{19}F (10–12) NMR spectra for 1–12 and CIF files giving crystallographic data for 6–8, 10, and 11. This material is available free of charge via the Internet at <http://pubs.acs.org>.

■ AUTHOR INFORMATION

Corresponding Author

*E-mail: andyhor@nus.edu.sg (T.S.A.H.); zhangw@imre.a-star.edu.sg (W.-H.Z.); zpliu@fudan.edu.cn (Z.-P.L.); david.young@ubd.edu.bn (D.J.Y.).

Author Contributions

#These authors contributed equally to this work.

Notes

The authors declare no competing financial interest.

■ ACKNOWLEDGMENTS

This work was supported by IMRE assured funding (10-1C0212); D.J.Y. acknowledges funding from Universiti Brunei Darussalam. We are grateful to the NUS and IMRE for support as well as Dr. Jonathan Hobley (IMRE) and the reviewers for their insightful discussion and comments.

■ REFERENCES

- (1) Zhang, W. H.; Hu, J.; Young, D. J.; Hor, T. S. A. *Organometallics* **2011**, *30*, 2137.
- (2) Zhang, W. H.; Zhang, X. H.; Tan, A. L.; Yong, M. A.; Young, D. J.; Hor, T. S. A. *Organometallics* **2012**, *31*, 553.
- (3) Bohne, C.; Abuin, E. B.; Scaiano, J. C. *J. Am. Chem. Soc.* **1990**, *112*, 4226.
- (4) Baldo, M. A.; Adachi, C.; Forrest, S. R. *Phys. Rev. B* **2000**, *62*, 10967.
- (5) Yakutkin, V.; Aleshchenkov, S.; Chernov, S.; Miteva, T.; Nelles, G.; Cheprakov, A.; Balushev, S. *Chem. Eur. J.* **2008**, *14*, 9846.
- (6) Singh-Rachford, T. N.; Castellano, F. N. *Coord. Chem. Rev.* **2010**, *254*, 2560.
- (7) Lamansky, S.; Djurovich, P.; Murphy, D.; Abdel-Razzaq, F.; Kwong, R.; Tsyba, I.; Bortz, M.; Mui, B.; Bau, R.; Thompson, M. E. *Inorg. Chem.* **2001**, *40*, 1704.
- (8) Lamansky, S.; Djurovich, P.; Murphy, D.; Abdel-Razzaq, F.; Lee, H.-E.; Adachi, C.; Burrows, P. E.; Forrest, S. R.; Thompson, M. E. *J. Am. Chem. Soc.* **2001**, *123*, 4304.
- (9) Rao, Y. L.; Schoenmakers, D.; Chang, Y. L.; Lu, J. S.; Lu, Z. H.; Kang, Y.; Wang, S. *Chem. Eur. J.* **2012**, *18*, 11306.
- (10) Chang, C. F.; Cheng, Y. M.; Chi, Y.; Chiu, Y. C.; Lin, C. C.; Lee, G. H.; Chou, P. T.; Chen, C. C.; Chang, C. H.; Wu, C. C. *Angew. Chem., Int. Ed.* **2008**, *47*, 4542.
- (11) Zhou, G.; Wong, W. Y.; Yang, X. *Chem. Asian J.* **2011**, *6*, 1706.
- (12) Du, B. S.; Liao, J. L.; Huang, M. H.; Lin, C. H.; Lin, H. W.; Chi, Y.; Pan, H. A.; Fan, G. L.; Wong, K. T.; Lee, G. H.; Chou, P. T. *Adv. Funct. Mater.* **2012**, *22*, 3491.
- (13) Farinola, G. M.; Ragni, R. *Chem. Soc. Rev.* **2011**, *40*, 3467.
- (14) Wu, C.; Chen, H. F.; Wong, K. T.; Thompson, M. E. *J. Am. Chem. Soc.* **2010**, *132*, 3133.
- (15) Reineke, S.; Lindner, F.; Schwartz, G.; Seidler, N.; Walzer, K.; Lüssem, B.; Leo, K. *Nature* **2009**, *459*, 234.
- (16) Adachi, C.; Baldo, M. A.; Thompson, M. E.; Forrest, S. R. *J. Appl. Phys.* **2001**, *90*, 5048.
- (17) Lee, S. J.; Park, J. S.; Song, M.; Shin, I. A.; Kim, Y. I.; Lee, J. W.; Kang, J. W.; Gal, Y. S.; Kang, S.; Lee, J. Y.; Jung, S. H.; Kim, H. S.; Chae, M. Y.; Jin, S. H. *Adv. Funct. Mater.* **2009**, *19*, 2205.
- (18) Tang, C. W.; Vanslyke, S. A. *Appl. Phys. Lett.* **1987**, *51*, 913.
- (19) Yersin, H. *Top. Curr. Chem.* **2004**, *241*, 1.
- (20) Thompson, M. E.; Djurovich, P. I.; Barlow, S.; Marder, S. R. In *Comprehensive Organometallic Chemistry*; O'Hare, D., Ed.; Elsevier: Oxford, U.K., 2007; Vol. 12, p 101.
- (21) Burn, P. L.; Lo, S. C.; Samuel, I. D. W. *Adv. Mater.* **2007**, *19*, 1675.
- (22) Chi, Y.; Chou, P. T. *Chem. Soc. Rev.* **2010**, *39*, 638.
- (23) You, Y.; Park, S. Y. *Dalton Trans.* **2009**, 1267.
- (24) Lowry, M. S.; Bernhard, S. *Chem. Eur. J.* **2006**, *12*, 7970.

- (25) Jiang, J.; Xu, Y.; Yang, W.; Guan, R.; Liu, Z.; Zhen, H.; Cao, Y. *Adv. Mater.* **2006**, *18*, 1769.
- (26) Lu, W.; Mi, B. X.; Chan, M. C. W.; Hui, Z.; Che, C. M.; Zhu, N.; Lee, S. T. *J. Am. Chem. Soc.* **2004**, *126*, 4958.
- (27) Wong, W. Y.; Ho, C. L. *Acc. Chem. Res.* **2010**, *43*, 1246.
- (28) Chen, F. F.; Chen, Z. Q.; Bian, Z. Q.; Huang, C. H. *Coord. Chem. Rev.* **2010**, *254*, 991.
- (29) Au, V. K. M.; Wong, K. M. C.; Tsang, D. P. K.; Chan, M. Y.; Zhu, N.; Yam, V. W. W. *J. Am. Chem. Soc.* **2010**, *132*, 14273.
- (30) Lo, S. C.; Burn, P. L. *Chem. Rev.* **2007**, *107*, 1097.
- (31) Costa, R. D.; Ortí, E.; Bolink, H. J.; Monti, F.; Accorsi, G.; Armaroli, N. *Angew. Chem., Int. Ed.* **2012**, *51*, 8178.
- (32) Su, H. C.; Chen, H. F.; Fang, F. C.; Liu, C. C.; Wu, C. C.; Wong, K. T.; Liu, Y. H.; Peng, S. M. *J. Am. Chem. Soc.* **2008**, *130*, 3413.
- (33) Wu, K. L.; Ho, S. T.; Chou, C. C.; Chang, Y. C.; Pan, H. A.; Chi, Y.; Chou, P. T. *Angew. Chem., Int. Ed.* **2012**, *51*, 5642.
- (34) He, L.; Qiao, J.; Duan, L.; Dong, G.; Zhang, D.; Wang, L.; Qiu, Y. *Adv. Funct. Mater.* **2009**, *19*, 2950.
- (35) Su, H. C.; Fang, F. C.; Hwu, T. Y.; Hsieh, H. H.; Chen, H. F.; Lee, G. H.; Peng, S. M.; Wong, K. T.; Wu, C. C. *Adv. Funct. Mater.* **2007**, *17*, 1019.
- (36) Bolink, H. J.; Coronado, E.; Costa, R. D.; Ortí, E.; Sessolo, M.; Graber, S.; Doyle, K.; Neuburger, M.; Housecroft, C. E.; Constable, E. C. *Adv. Mater.* **2008**, *20*, 3910.
- (37) Nazeeruddin, M. K.; Humphry-Baker, R.; Berner, D.; Rivier, S.; Zuppiroli, L.; Grätzel, M. *J. Am. Chem. Soc.* **2003**, *125*, 8790.
- (38) Gao, R.; Ho, D. G.; Hernandez, B.; Selke, M.; Murphy, D. L.; Djurovich, P. I.; Thompson, M. E. *J. Am. Chem. Soc.* **2002**, *124*, 14828.
- (39) You, Y.; Park, S. Y. *Adv. Mater.* **2008**, *20*, 3820.
- (40) Zeng, H.; Yu, F.; Dai, J.; Sun, H.; Lu, Z.; Li, M.; Jiang, Q.; Huang, Y. *Dalton Trans.* **2012**, *41*, 4878.
- (41) Schmitt, M.; Lin, H. *Inorg. Chem.* **2007**, *46*, 9139.
- (42) Zhao, Q.; Liu, S. J.; Li, F. Y.; Yi, T.; Huang, C. H. *Dalton Trans.* **2008**, 3836.
- (43) Mak, C. S. K.; Pentlechner, D.; Stich, M.; Wolfbeis, O. S.; Chan, W. K.; Yersin, H. *Chem. Mater.* **2009**, *21*, 2173.
- (44) Xie, Z.; Ma, L.; deKrafft, K. E.; Jin, A.; Lin, W. *J. Am. Chem. Soc.* **2009**, *132*, 922.
- (45) Lee, P. K.; Law, W. H. T.; Liu, H. W.; Lo, K. K. W. *Inorg. Chem.* **2011**, *50*, 8570.
- (46) Lo, K. K. W.; Zhang, K. Y.; Leung, S. K.; Tang, M. C. *Angew. Chem., Int. Ed.* **2008**, *47*, 2213.
- (47) Yang, Y.; Zhao, Q.; Feng, W.; Li, F. *Chem. Rev.* **2013**, *113*, 192.
- (48) You, Y.; Nam, W. *Chem. Soc. Rev.* **2012**, *41*, 7061.
- (49) Hull, J. F.; Balcells, D.; Blakemore, J. D.; Incarvito, C. D.; Eisenstein, O.; Brudvig, G. W.; Crabtree, R. H. *J. Am. Chem. Soc.* **2009**, *131*, 8730.
- (50) Werner, H. *Angew. Chem., Int. Ed.* **2010**, *49*, 4714.
- (51) Condie, A. G.; González-Gómez, J. C.; Stephenson, C. R. J. *J. Am. Chem. Soc.* **2010**, *132*, 1464.
- (52) Nagib, D. A.; MacMillan, D. W. C. *Nature* **2011**, *480*, 224.
- (53) Nagib, D. A.; Scott, M. E.; MacMillan, D. W. C. *J. Am. Chem. Soc.* **2009**, *131*, 10875.
- (54) Kent, C. A.; Liu, D.; Meyer, T. J.; Lin, W. *J. Am. Chem. Soc.* **2012**, *134*, 3991.
- (55) Kent, C. A.; Mehl, B. P.; Ma, L.; Papanikolas, J. M.; Meyer, T. J.; Lin, W. *J. Am. Chem. Soc.* **2010**, *132*, 12767.
- (56) Wang, C.; Lin, W. *J. Am. Chem. Soc.* **2011**, *133*, 4232.
- (57) van Leeuwen, P. W. N. M.; Kamer, P. C. J.; Reek, J. N. H.; Dierkes, P. *Chem. Rev.* **2000**, *100*, 2741.
- (58) Marimuthu, T.; Bala, M. D.; Friedrich, H. B. *J. Coord. Chem.* **2009**, *62*, 1407.
- (59) Ricken, S.; Osinski, P. W.; Eilbracht, P.; Haag, R. *J. Mol. Catal. A: Chem.* **2006**, *257*, 78.
- (60) Dallanegra, R.; Chaplin, A. B.; Weller, A. S. *Organometallics* **2012**, *31*, 2720.
- (61) Williams, G. L.; Parks, C. M.; Smith, C. R.; Adams, H.; Haynes, A.; Meijer, A. J. H. M.; Sunley, G. J.; Gaemers, S. *Organometallics* **2011**, *30*, 6166.
- (62) Pontiggia, A. J.; Chaplin, A. B.; Weller, A. S. *J. Organomet. Chem.* **2011**, *696*, 2870.
- (63) Smith, C. S.; Branham, C. W.; Marquardt, B. J.; Mann, K. R. *J. Am. Chem. Soc.* **2010**, *132*, 14079.
- (64) Yu, M. X.; Zhao, Q.; Shi, L. X.; Li, F. Y.; Zhou, Z. G.; Yang, H.; Yia, T.; Huang, C. H. *Chem. Commun.* **2008**, 2115.
- (65) Lin, C. H.; Lin, C. Y.; Hung, J. Y.; Chang, Y. Y.; Chi, Y.; Chung, M. W.; Chang, Y. C.; Liu, C.; Pan, H. A.; Lee, G. H.; Chou, P. T. *Inorg. Chem.* **2012**, *51*, 1785.
- (66) van der Veen, L. A.; Keeven, P. H.; Schoemaker, G. C.; Reek, J. N. H.; Kamer, P. C. J.; van Leeuwen, P. W. N. M.; Lutz, M.; Spek, A. L. *Organometallics* **2000**, *19*, 872.
- (67) Fox, D. J.; Duckett, S. B.; Flaschenriem, C.; Brennessel, W. W.; Schneider, J.; Gunay, A.; Eisenberg, R. *Inorg. Chem.* **2006**, *45*, 7197.
- (68) Tamayo, A. B.; Alleyne, B. D.; Djurovich, P. I.; Lamansky, S.; Tsyba, I.; Ho, N. N.; Bau, R.; Thompson, M. E. *J. Am. Chem. Soc.* **2003**, *125*, 7377.
- (69) Thomas, K. R. J.; Velusamy, M.; Lin, J. T.; Chien, C. H.; Tao, Y. T.; Wen, Y. S.; Hu, Y. H.; Chou, P. T. *Inorg. Chem.* **2005**, *44*, 5677.
- (70) Yang, W.; Zhang, S.; Ding, Y.; Shi, L.; Song, Q. *Chem. Commun.* **2011**, *47*, 5310.
- (71) Wang, X. Y.; Kimyonok, A.; Weck, M. *Chem. Commun.* **2006**, 3933.
- (72) Zhao, Q.; Jiang, C. Y.; Shi, M.; Li, F. Y.; Yi, T.; Cao, Y.; Huang, C. H. *Organometallics* **2006**, *25*, 3631.
- (73) Tsuboyama, A.; Iwawaki, H.; Furugori, M.; Mukaide, T.; Kamatani, J.; Igawa, S.; Moriyama, T.; Miura, S.; Takiguchi, T.; Okada, S.; Hoshino, M.; Ueno, K. *J. Am. Chem. Soc.* **2003**, *125*, 12971.
- (74) King, K. A.; Spellane, P. J.; Watts, R. J. *J. Am. Chem. Soc.* **1985**, *107*, 1431.
- (75) Chou, P. T.; Chi, Y. *Eur. J. Chem.* **2007**, *13*, 380.
- (76) Li, J.; Djurovich, P. I.; Alleyne, B. D.; Yousufuddin, M. Y.; Ho, N. N.; Thomas, J. C.; Peters, J. C.; Bau, R.; Thompson, M. E. *Inorg. Chem.* **2004**, *44*, 1713.
- (77) Lin, C. H.; Chang, Y. Y.; Hung, J. Y.; Lin, C. Y.; Chi, Y.; Chung, M. W.; Lin, C. L.; Chou, P. T.; Lee, G. H.; Chang, C. H.; Lin, W. C. *Angew. Chem., Int. Ed.* **2011**, *50*, 3182.
- (78) Soler, J. M.; Artacho, E.; Gale, J. D.; García, A.; Junquera, J.; Ordejón, P.; Sanchez-Portal, D. S. *J. Phys.: Condens. Matter* **2002**, *14*, 2745.
- (79) Shang, C.; Liu, Z. P. *J. Am. Chem. Soc.* **2011**, *133*, 9938.
- (80) Suppan, P. *J. Chem. Soc., Faraday Trans. 1* **1986**, *82*, 509.
- (81) Sohn, H.; Sailor, M. J.; Magde, D.; Troglor, W. C. *J. Am. Chem. Soc.* **2003**, *125*, 3821.
- (82) Demas, J. N.; Crosby, G. A. *J. Phys. Chem.* **1971**, *75*, 991.
- (83) Sheldrick, G. M. *SADABS. Program for empirical absorption correction of area detector data*; University of Göttingen, Göttingen, Germany, 1996.
- (84) Sheldrick, G. M. *SHELXS-97 and SHELXL-97. Programs for crystal structure solution and refinement*; University of Göttingen, Göttingen, Germany, 1997.